

The impact of an extreme cloud burst on Edinburgh Castle

Article

Published Version

Creative Commons: Attribution 4.0 (CC-BY)

Open Access

Tett, S. F. B., Cha, Y., Donovan, K., Geffers, G.-M. and Hawkins, E. ORCID: <https://orcid.org/0000-0001-9477-3677> (2023) The impact of an extreme cloud burst on Edinburgh Castle. *Bulletin of the American Meteorological Society*, 104 (10). E1807-E1816. ISSN 1520-0477 doi: <https://doi.org/10.1175/BAMS-D-22-0196.1> Available at <https://centaur.reading.ac.uk/113861/>

It is advisable to refer to the publisher's version if you intend to cite from the work. See [Guidance on citing](#).

To link to this article DOI: <http://dx.doi.org/10.1175/BAMS-D-22-0196.1>

Publisher: American Meteorological Society

All outputs in CentAUR are protected by Intellectual Property Rights law, including copyright law. Copyright and IPR is retained by the creators or other copyright holders. Terms and conditions for use of this material are defined in the [End User Agreement](#).

www.reading.ac.uk/centaur

CentAUR

Central Archive at the University of Reading

Reading's research outputs online

The Impact of an Extreme Cloud burst on Edinburgh Castle

Simon F. B. Tett, YoungHwa Cha, Kate Donovan,
Gina-Maria Geffers, and Ed Hawkins

An extreme cloudburst on 4 July 2021 damaged Edinburgh Castle. Relative to preindustrial, and based on results from a convective permitting model, observed warming increased the risk by ~30%, which further increases to ~70% in a +2-K world.

On 4 July 2021, a band of high-intensity rain tracked across the city of Edinburgh, Scotland, releasing an intense downpour (“cloudburst”) directly over Edinburgh Castle for about 15 min. Staff at the castle reported that the rainfall was unprecedented. The Royal Botanic Gardens Edinburgh (RBGE) weather station, a kilometer to the north of the castle, recorded a daily rainfall of 57.6 mm, about 80% of the month’s average rainfall of 72.1 mm. This rainfall event also led to considerable surface water flooding across the city (BBC News 2021). Scottish climate has warmed by about 1 K since the late nineteenth century (Kendon et al. 2022) though with only modest changes in total summer rainfall since then (www.metoffice.gov.uk/research/climate/maps-and-data/uk-temperature-rainfall-and-sunshine-time-series).

Heritage organizations are adapting to climate change, including extreme weather events, with a few record-event damage cases making it difficult to estimate climate risk (Historic Environment Scotland 2019; Phillips 2014). There are only a small number of studies in earlier *BAMS* special reports on daily

AFFILIATIONS: Tett, Cha, Donovan, and Geffers—School of Geosciences, University of Edinburgh, Edinburgh, United Kingdom; Hawkins—National Centre for Atmospheric Science, Department of Meteorology, University of Reading, Reading, United Kingdom


DOI: <https://doi.org/10.1175/BAMS-D-22-0196.1>

CORRESPONDING AUTHOR: Simon F. B. Tett, simon.tett@ed.ac.uk

Supplemental material: <https://doi.org/10.1175/BAMS-D-22-0196.2>

In final form 11 April 2023

© 2023 American Meteorological Society. This published article is licensed under the terms of a Creative Commons Attribution 4.0 International

(CC BY 4.0) License 

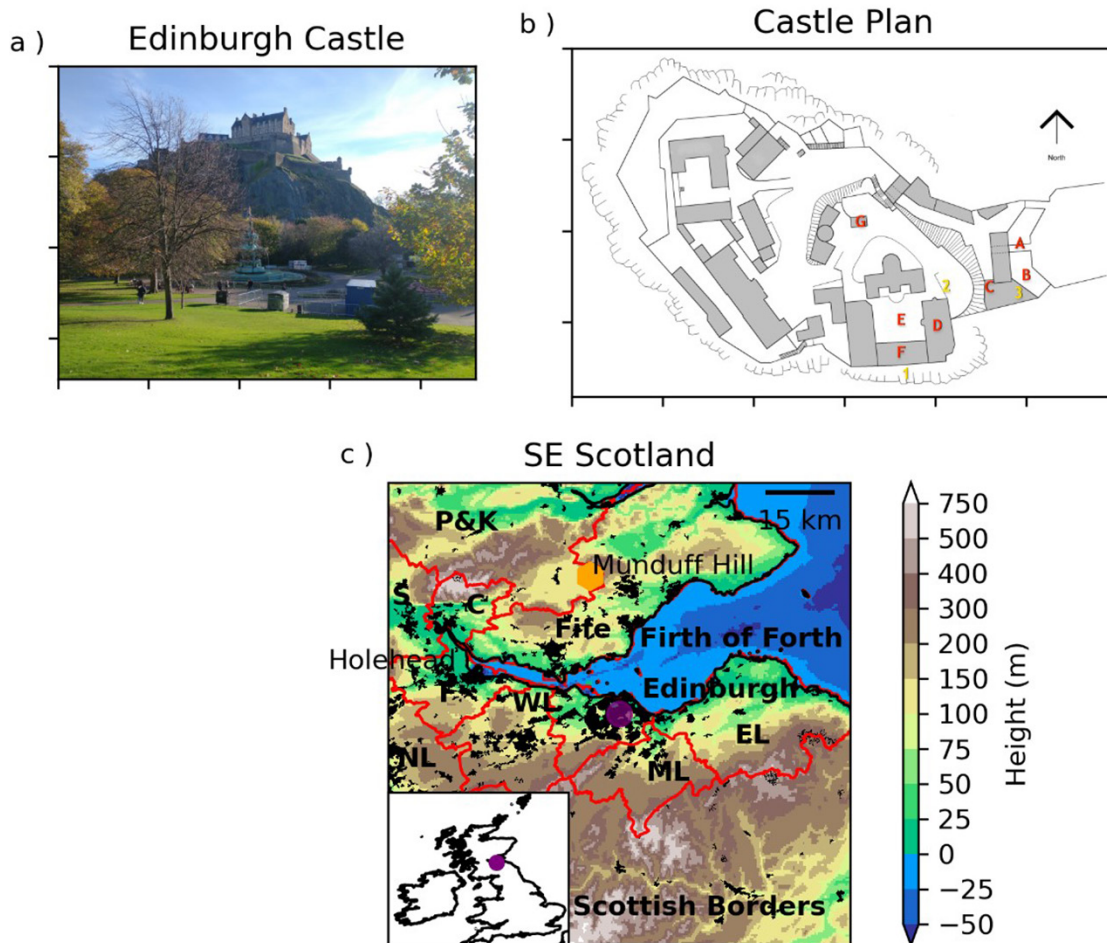


Fig. 1. (a) Photograph of Edinburgh Castle taken from the north. (b) Plan of the castle complex (modified from https://commons.wikimedia.org/wiki/File:Edinburgh_Castle_Plan.png): A = Drawbridge (main entrance), B = Exercise Yard, C = Main visitor's toilet, D = Royal Palace (Mary Room and Laich Hall), E = Crown Square, F = Great Hall (Stick Room), G = Saint Margaret's Chapel. Plant room locations: 1 = Devil's elbow, 2 = David's tower, 3 = Exercise Yard plant room. (c) Southeast Scotland. Inset map shows position of Edinburgh (purple circle) within the British Isles. Main plot shows topography (color bar to the right) in the Edinburgh region. Black shows urban areas. Orange hexagon shows the location of Munduff Hill radar station. Red lines show boundaries of local authorities. S = Stirling, WL, ML, EL = West, Mid, and East Lothian, respectively. Purple dot is the location of the castle.

extremes and a very limited number of studies that consider attribution of subdaily rainfall. Reed et al. (2022), building on Reed et al. (2021), examined changes in extreme 3-hourly precipitation in the 2020 North Atlantic hurricane season finding that human influences had increased extreme rainfall intensity by about 10% per 1 K of warming. The National Academies of Sciences, Engineering, and Medicine (2016) report suggests low confidence in understanding and attribution of severe convective storms and modest confidence in extreme rainfall. Our study fills these research gaps by describing the impact of the 2021 event on the castle and estimates how climate change has impacted the probability and intensity of the event for improved decision-making.

Edinburgh Castle is in the center of Edinburgh, at the top of an eroded volcanic plug and dominates the urban landscape (Fig. 1a). The castle is about 130 m above average sea level and up to 80 m above the local ground level (Historic Environment Scotland 2020). Thus, the main flooding risk to the castle is from heavy short duration rainfall. Much of Edinburgh city

center is a UNESCO World Heritage Site, with the castle being one of the largest heritage sites in the city and of significant cultural and economic value. It is one of the oldest fortified sites in Europe and is made up of several buildings (Fig. 1b) with the oldest being Saint Margaret's Chapel (label G) constructed in the twelfth century.

At 1200 UTC 4 July 2021 (Royal Meteorological Society 2021) there was a low pressure system to the west of Ireland, and a convergence line centered over western Scotland and northern England (Royal Meteorological Society 2021). By 5 July 2021, the convergence line had dissipated and the low had moved westward and filled. Five-minute radar rainfall shows a line of rainfall extending from Stirling, West Lothian, and into the Scottish borders at 1500 British summer time (BST; BST = GMT + 1 h; Fig. 2a), likely the position of the eastward-moving convergence line. Throughout most of the line, radar rainfall is around 10 mm h^{-1} with small regions of intense rainfall. Note in particular the feature in West Lothian to the west of Edinburgh. An hour later, the rain line has moved east and broadened with very heavy rainfall rates over Edinburgh (Fig. 2b). By 1700 BST (Fig. 2c) the rain line is beginning to disperse, though still with heavy rain in Fife. The rainfall at two sites in Edinburgh (Fig. 2d) is short duration, with the majority of the rainfall occurring in about 15 min, at around 1600 BST, with peak rates at the RBGE of 140 mm h^{-1} . Total radar rainfall is 32 and 35 mm at the castle and RBGE, respectively. Total radar rainfall is 32 and 35 mm at the castle and RBGE, respectively.

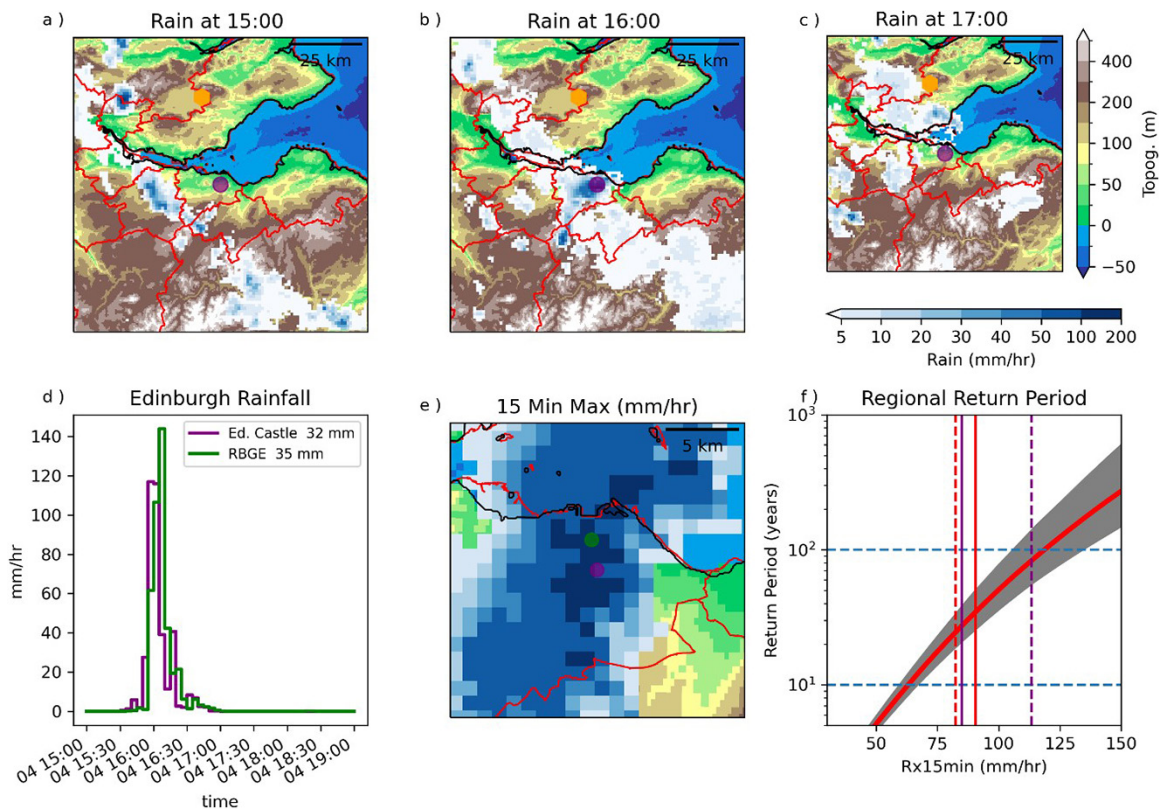


Fig. 2. (a)–(c) The 5-min radar rainfall rate (mm h^{-1}) at 1500, 1600, and 1700 British summer time plotted over topography for SE Scotland. Only rainfall rates $> 1 \text{ mm h}^{-1}$ are shown. Orange hexagon shows the location of the Munduff Hill radar station. Rainfall scale is quasi logarithmic and is shown below (c). Topography scale is shown to the right of (c). (d) The 5-min radar rainfall rates at Edinburgh Castle (purple) and RBGE (green). (e) Maximum 15-min rain (Rx15min) on $20 \text{ km} \times 20 \text{ km}$ region centered on Edinburgh Castle for 4 Jul 2021. Only rates $> 10 \text{ mm h}^{-1}$ are shown. Green dot shows the location of RBGE. Purple circle in (a)–(c) and (e) shows location of Edinburgh Castle while red lines show local authority boundaries. See Fig. 1c for details. (f) Summer Rx15min (mm h^{-1}) from regional analysis using 95th quantile (see methods) for GEV fit (red line) and 5%–95% uncertainty (gray region). Solid and dashed vertical purple (red) lines show regional 95% (castle) Rx15min for 2021 and 2020, respectively. The castle rainfall is the radar rainfall recorded at the castle location.

In the rest of this paper, we focus on the maximum radar rainfall rate (mm h^{-1}) in a 15-min period (Rx15min), generally during summer (JJA). Daily Rx15min, for 4 July (Fig. 2e), is largest in a north–south line about 10 km wide with considerable variation within that on the kilometer scale. JJA 2021 Rx15min, at the castle, occurred on 4 July and was 90.8 mm h^{-1} . Using all appropriate radar data (see methods) from 2005 to 2020 inclusive this is a roughly 1-in-120-yr event. In August 2020 an extreme rainfall event also impacted Edinburgh, though the heaviest rain was in Fife (Scottish Environment Protection Agency 2020) with a JJA castle Rx15min of 78.4 mm h^{-1} occurring on 11 August 2020. The return period of regional extremes (see methods) was about 30 and 100 years for 2021 and 2020, respectively (Fig. 2f), suggesting both are unusual events.

Data, methods, and event definition

The impacts on the castle were captured using qualitative data from semistructured interviews. Between 21 January and 1 February 2022, 10 interviews with Historic Environment Scotland staff responsible for Edinburgh Castle were conducted. The damage and losses were categorized including impacts on the site operations such as income, maintenance costs, staff working hours, and external contractors and staff and visitors’ health and safety (Table 1).

The extreme rainfall at Edinburgh Castle was a “cloudburst” occurring on a 15-min–1-km scale. As part of the U.K. Climate Projections (UKCP) project (Met Office Hadley Centre 2019) an ensemble of convection permitting model (CPM) simulations were carried out. The model resolution is 2.2 km and only hourly data are available from the diagnostics so we cannot directly use model data to estimate the change in probability or rainfall intensity of the “cloudburst.” Instead, we first use radar data to estimate the current cumulative distribution function (CDF) of regional summer Rx15min. We then adjust this radar distribution based on the sensitivity of simulated CPM summer maximum hourly rainfall (Rx1hr) to central England temperature (CET) values (see below). This gives estimates of the CDF of regional maximum summer rainfall at various CET values. From these CDFs we compute probability and intensity ratios, relative to preindustrial, of seasonal Rx15min.

To estimate the change in radar Rx15min due to climate change we use seasonal hourly extreme (Rx1hr) from the CPM simulations for which time slices for 1980–2000, 2020–40, and 2060–80 were run (see online supplemental material for a broader discussion of this; <https://doi.org/10.1175/BAMS-D-22-0196.2>). Boundary conditions from an ensemble of 12 global climate models (Yamazaki et al. 2021) drove a 12-km regional model, which in turn drove the 2.2-km CPM. The driving global models have a high climate sensitivity and likely warm too much (Tokarska et al. 2020; Yamazaki et al. 2021). We use extreme value theory (Coles 2001) with covariates to estimate extreme distributions as a function of the covariate (see supplemental material for more detail). We do this by fitting, at each point in the region, a generalized extreme value (GEV) distribution, with a covariate (Gilleland and Katz 2016) for the scale and location parameters, to Rx1hr. The region considered is an approximately $100 \text{ km} \times 100 \text{ km}$ region centered on Edinburgh Castle. We explored four different covariates:

Table 1. Color coding criteria for damage and loss: minor, moderate, and severe.

	Damage	Loss
	Business as usual	Within regular maintenance costs
Minor	Minor: Only cleaning required	Out of contracted hours/volunteer, small emergency purchases, additional HR costs
Moderate	Moderate: Partial repair required, limited access	High opportunity costs and potential additional resources required
Severe	Severe: Major operation required or causing site closure	Impact on safety, major economic and monuments losses, or required major salvaging collections

CET (Parker and Horton 2005), regional temperature, saturated humidity computed from the monthly time series of regional temperature, and average temperature across the whole CPM domain. Average Akaike information criterion (AIC) for the fits, over the Edinburgh region, are 4,737, 4,721, 4,726, and 4,729 for CET, the whole CPM region, regional temperatures, and regional humidity, respectively. The average AIC with no covariate is 4,772 suggesting that the statistical model with covariate is better than one without. We used CET as a covariate as it is a long instrumental series and the observed warming has been attributed to anthropogenic forcing (Karoly and Stott 2006). To explore sensitivity to rain time period we also computed summer Rx2hr, Rx4hr, and Rx8hr from the CPM simulations and repeated our analysis. We also repeated our analysis where we also used CET as a covariate for the shape parameter (see supplemental material).

Regressing CET on regional saturated humidity from the CPM gives $6.1\% \pm 0.05\% \text{ K}^{-1}$ (Fig. S1a in the online supplemental material), smaller than the expected $7\% \text{ K}^{-1}$ (Allen and Ingram 2002). This is because regional temperatures warm at 0.84 ± 0.006 of CET (Fig. S1b). These two relationships have an R^2 of 97%. Regional rainfall decreases with temperature while the regional median of Rx1hr increases, though both have a low R^2 value (Figs. S1c,d).

The scale and location parameters from the GEV fits are smallest over the sea and largest above 200 m (Figs. S3a,b) and relatively homogeneous in land regions below 200 m. Largest values occur at the edge of steep topography (Fig. 1c). Examining the fractional change in scale and location per degree CET change (Fig. S3c) clear differences can be seen between ocean grid points (dark blue) and regions above 200 m (yellow and brown). Considering only those points which have heights greater than 0 m (land) and less than 200 m, the scale changes are greater than Clausius–Clapeyron (CC), with the mean change being about 50% larger. Many grid points have percentage changes in location per 1 K CET warming less than the CC value with an average change of about 90% of CC. These sensitivity differences may be because, in the CPM, mean rainfall is declining so changes in the median Rx1hr are weaker than CC. QQ plots (Figs. S3e,f) for two points suggest that the covariate fit is adequate. Uncertainties in the mean fractional change are computed by bootstrapping (Efron and Tibshirani 1993) 1,000 times, though only sampling 1% of the appropriate CPM points to reduce the impact of extreme event correlation. Sampling uncertainties in the fractional parameter changes are relatively small (Fig. S3c).

Rain gauges are sparse (Yu et al. 2020) and so we use the United Kingdom's radar NIMROD data (Met Office 2003) which has corrections via comparison with gauge data. These data are available from mid-2005 to near present at a spatial resolution of 1 km and a temporal resolution of 5 min, although they likely underestimate extreme rainfall (Harrison et al. 2000). Data were quality controlled by setting any 5-min rates greater than 400 mm h^{-1} to missing. Fifteen-minute averages were computed by averaging the 5-min values with missing data ignored in the average. From this 15-min average at each $1 \text{ km} \times 1 \text{ km}$ cell the summer maximum (Rx15min) and time of maximum were computed, as well as the total summer rainfall. The radar at Munduff Hill (Fig. 1c) is about 30 km to the NW of Edinburgh with little topography between it and the low-lying land around the Firth of Forth suggesting that the data should be of high quality. Examining mean JJA total rainfall (Fig. S2) we see only a few radar artifacts at high topography. The mean JJA Rx15min radar rainfall also shows few apparent artifacts. Examining the distribution of both total JJA rainfall (for each year and cell) there appears to be a few cases of rainfall greater than 1,000 mm in a season. We remove such seasons and locations from the Rx15min data.

To estimate the distribution for radar rain extremes from the radar data, following Saltikoff et al. (2019), we treat space and time as exchangeable. Based on the CPM results we only consider data with height $> 0 \text{ m}$ (land) and $\leq 200 \text{ m}$. However, to fit distributions, we need

independent data. We define an event as all summer Rx15min that occur in the same 12-h period either 0000–1200 BST or 1200–0000 BST giving a maximum of two events per day or 184 events per summer. We further require that the event has at least 25 Rx15min in the same 12-h period, which means it is at least 25 km² in size. We end up with 384 events for 2005–20. For each event, from the Rx15min values, we compute spatial quantiles, largely focusing on the 95% but also considering the 5%, 10%, 20%, 50%, 80%, and 90% quantiles and fit a GEV to these values. Kolmogorov–Smirnov tests on each quantile are in the range 0.79–0.93, suggesting the fit is adequate, confirmed by Q–Q plots (Fig. S2d). Uncertainties in the GEV fit were computed by bootstrapping 1,000 times over the 384 events.

We estimate that summer CET increases at 0.94 ± 0.03 times the change in global annual average temperature using a simple regression between CET and HadCRUT5 (Morice et al. 2021), following the approach in Hawkins et al. (2020) where the global temperature is smoothed with a 41-yr lowess filter and CET is lightly smoothed with an 11-yr lowess filter. We assume that summer CET would be 1.88 ± 0.06 K warmer in a +2-K world. When computing changes in CET at +2 K, we randomly sample from this distribution.

Return values for the GEV increase by a factor r if the location and scale parameters increase by a factor r (supplemental material). Motivated by this, we compute the GEV CDF of radar regional extremes, at specified CET values, by scaling the location and scale parameters by the average fractional scaling in the scale and location parameters, relative to 2005–20, from the fit CPM GEV. This assumes that fractional changes in Rx15min are similar to changes in Rx1hr. The average scalings are computed from the 100 km \times 100 km region centered on Edinburgh Castle with height > 0 m and ≤ 200 m and mean CET for the period in question. From the adjusted regional extreme radar rain probabilities of exceeding rainfall thresholds and the change in intensity as a function of return time are computed. We then compute the ratios of these relative to the preindustrial distribution defined as the mean CET for 1850–99 (IPCC 2021). We compute intensity ratios (IR) and probability ratios (PR) for a range of return periods and Rx15min for three periods: 1980–89, 2012–21 (when the event happened), and preindustrial plus 2°. Uncertainties are computed by combining the bootstrapped scaling uncertainties and the radar fit uncertainties for which we report the 5%–95% uncertainty ranges shown to the nearest percent. For PI+2K, we also include uncertainty from the assumed Gaussian uncertainty.

Results

The most costly damage occurred in two rooms accessed from Crown Square (E in Fig. 1b) which is higher than most of the castle site. Surface water and discharged water from the roof ran down to the southeast corner of Crown Square, the drainage was overwhelmed and water overflowed the 15-cm step entrance into the Mary Room (D). Surface water also traveled down toward the main entrance of the castle, with some diverted into the main visitor's toilet. The water rose to approximately 50 cm within a 15-min period at the entrance to the visitor's toilet (C).

The damage and losses in the flooded rooms (the Mary Room and antechamber to Laich Hall) led to a 6-month recovery program and closure of these rooms to the public. The protection of historical collections within these rooms was paramount, and therefore, repair to the fabric of the room incurred indirect losses such as staff time. The castle site illustrates the multiple facets involved during a flood recovery program including welfare of the public, management of the collections, consistency of repair, as well as the need for external heritage experts monitoring and providing advice during repair (Table 2). The complexity of repairing just two rooms in a large complex highlights the need for improved preplanning for extreme rainfall events, including a review of key drainage points which were overwhelmed. Visitor numbers were low

Table 2. Damage and loss identified at the castle categorized as minor (yellow), moderate (orange), or severe (red). See Table 1 for description of categories. N/A means no damage or loss or have not reported.

	Damage		Loss		
	Direct	Indirect	Direct cost	Staff time	Safety ^a
Building outdoor fabrics	Overflow of gutters and roofs	No water into inside from roofs, downpipes, and gutters	N/A	Extra cleaning hours	No injured staff or visitors
Building indoor fabrics	Mary Room and main visitors toilet flooded	Increased threat of mold due to humidity	Carpet replacement in Mary Room	Extra cleaning, monitoring hours	N/A
Drainage system	Drainage overwhelmed. Water rose 15 cm at the southeast corner of Crown Square and 50 cm at main visitors toilet, some water with debris at the Exercise Yard.		N/A ^b	Extra cleaning hours	N/A
Plant rooms	Water ingress but no issues	N/A	Gas meters	Extra cleaning hours	N/A
Collections	No damage to collections	No mold developments, no reputational risks	Two or more dehumidifiers	1–2 weeks of intensive monitoring, inspections and coordination over 6 months+	N/A
Pavements	Cobbles, infills were washed away	N/A	Pavement infills	Contractor hours	N/A
Site operation	Early closure	No significant impact on ticket sale	No refund costs	N/A	N/A ^c

^a Safety refers to staff and visitors' well-being threatened by direct and indirect damages causing injuries and risk or danger to health.

^b No extra cost incurred. Clearing blockage to drainage is within maintenance coverage.

^c Minor note: visitors were told to exit out into the heavy rain in order to close the castle.

due to the COVID-19 pandemic and future extreme weather events should be prepared for with public welfare in mind. The surface water flow through the steep castle complex was rapid and at a potentially dangerous depth posing considerable risk to visitors and staff.

We estimate that the regional extreme was a 1-in-28-yr event with the castle Rx15min being slightly larger than this (Fig. 2f). The probability of having a rainfall extreme as large as happened at Edinburgh Castle, conditional on the 95th quantile of 80 mm h⁻¹, is about 5% giving a return time for the castle Rx15min of about 1-in-500 years. This is larger than the empirical estimate of about 1-in-120 years. Mindful of large uncertainties we estimate the castle event at a 1-in-100- to 1-in-1,000-yr event in today's climate.

IRs are fairly uniform over the return periods we consider and about 50% larger than Clausius–Clapeyron (Fig. 3a). For the 1980s, the regional event is 2% (2%–2%) larger than late-nineteenth-century values, for 2012–21, 8% (7%–9%) larger, and at +2K is 16% (14%–18%) larger. PRs generally increase with Rx15min but are significantly different from one for all Rx15min considered (Fig. 3b). For the regional Rx15min of approximately 80 mm h⁻¹ PR is 1.09 (1.07–1.11) during the 1980s, increases to 1.33 (1.27–1.41) for 2012–21, and is projected to increase to 1.72 (1.57–1.91) in the +2-K world. We repeated the analysis with Rx2hr, Rx4hr, and Rx8hr data finding a shift to smaller changes in intensity and probability ratios as the time scale lengthened (Figs. 3a,b). If this were to continue to Rx15min we would expect larger changes in PR and IR that we find from Rx1hr.

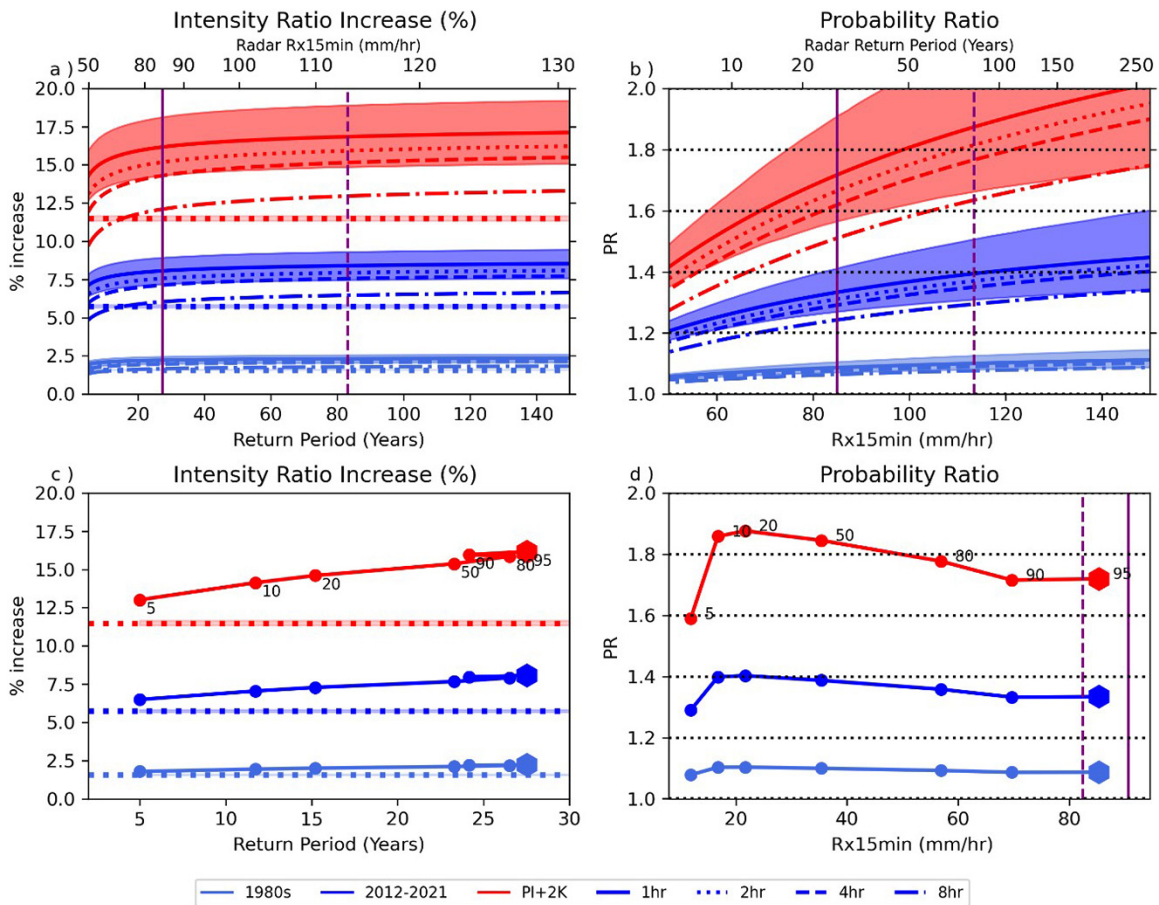


Fig. 3. (a) Intensity ratio increase (%) as function of return period and (b) probability ratio as function of regional Rx15min. Shown is best estimate (line) and 5%–95% uncertainty range (shading). Horizontal dotted lines in (a) show expected intensity change if extremes scale with Clausius–Clapeyron. The top axis in (a) and (b) shows the equivalent rainfall and return period estimated from the radar rainfall data while vertical purple lines show the regional rainfall maximum for 2020 (dashed) and 2021 (solid). Dotted, dashed, and dot–dashed lines in (a) and (b) show results when scaling is estimated from simulated 2-, 4-, and 8-hourly summer maxima (Rx2hr, Rx4hr, and Rx8hr). (c) Intensity ratio increase (%) as function of return period for best estimates using different quantiles (labels on PI+2K line) to define regional extreme. Hexagon markers show 95th quantile used in (a) and (b). (d) As in (c), but for probability ratio as function of Rx15min. Vertical purple lines show Edinburgh Castle Rx15min for 4 Jul 2021 (solid) and 11 Aug 2020 (dashed). Note these are different from the regional 95th quantiles shown in (a) and (b).

We consider sensitivity to the quantile within the regional extreme rainfall. Both Rx15min and return period change with quantile choice and IR generally increases with quantile (Fig. 3c). For all quantiles, considered values are larger than the CC value (Fig. 3c). Probability ratios are, except for the 5%, not very sensitive to quantile though do show a slight decline with increasing quantile (Fig. 3d).

We repeated our analysis with the shape parameter also varying with CET (Fig. S4). We find uncertainties in IR and PR a little larger and best estimates a little smaller than with a fixed shape parameter.

Conclusions

We find an increase in rainfall intensity at fixed return periods, due to warming since the late nineteenth century, about 50% larger than expected from Clausius–Clapeyron. The probability of an event similar to that which occurred in July 2021 is about 30% larger due

to this warming and about 70% larger in a world 2 K warmer than preindustrial. Sampling uncertainties in our CPM analysis are small, but we did not consider the likely considerable uncertainty arising from different CPM systems nor on the relationship between hourly and 15-min regional extremes or 2.2-km-resolution models and the few-kilometer scale of the event. Pichelli et al. (2021), using an ensemble of 12 models driven by SSTs taken from global models, and an Alpine domain found that 99.9% hourly rainfall was, on average, reduced by about 10%, relative to 1996–2005. They found very large uncertainties with a 5%–95% range of about –35% to +15%. Some of this range could arise from the likely very different drivers of the models but much likely arises from the different CPMs used suggesting sensitivity to details of the CPM.

The impact of the extreme rainfall event on Edinburgh Castle was relatively minimal, yet when water pooled and flowed into some of the publicly accessible rooms the process of repair was lengthy due to the distinctive conservation needs. The most significant loss was in staff time, while the relatively low visitor numbers during the pandemic reduced the risk to the general public substantially.

The qualitative damage narratives were combined with the quantitative attribution results via “what if” scenarios. These scenarios took into account possible different climate futures, the influence of the COVID-19 pandemic, and the timing of the event itself. Combining these data through descriptive scenarios provided heritage managers with risk narratives. They were then able to identify two options that would have reduced the impact of such an event: 1) an accurate nowcasting system with appropriate people-centered early warning protocols in place and 2) an increased capacity of the drainage systems in Crown Square. At the time of writing Historic Environment Scotland had not implemented either of these recommendations.

Our research demonstrates the value of cross-disciplinary collaboration for risk management. Bringing attribution scientists together with interdisciplinary risk researchers and key stakeholders led to the development of integrated evidence for risk management as well as recommendations for postevent damage surveys. Working together, we were able to identify critical data necessary for decision-making and for improving future attribution studies.

Acknowledgments. SFBT, KD, GMG, and YC were funded by National Centre for Resilience and Historic Environment Scotland. The authors thank all contributors to this project, including staff members across Historic Environment Scotland and their partners and are very grateful to David Harkin. SFBT was also funded by Grant AH/V006398/1, and EH was supported by the National Centre for Atmospheric Science and NERC GloSAT project. Thanks to J. Tett for the photograph of Edinburgh Castle. We thank the two anonymous reviewers for their comments which considerably improved the manuscript.

Data availability statement. Software and data used in the probabilistic analysis are available from <https://doi.org/10.5281/zenodo.7437991> and <https://doi.org/10.7488/ds/3788>, respectively. Interview data are available upon request to KD.

References

- Allen, M. R., and W. J. Ingram, 2002: Constraints on future changes in climate and the hydrologic cycle. *Nature*, **419**, 224–232, <https://doi.org/10.1038/nature01092>.
- BBC News, 2021: Edinburgh flooding: Half of July rain fell in one hour. BBC News, www.bbc.co.uk/news/uk-scotland-edinburgh-east-fife-57718384.
- Coles, S., 2001: *An Introduction to Statistical Modeling of Extreme Values*. Springer, 208 pp.
- Efron, B., and R. J. Tibshirani, 1993: *An Introduction to the Bootstrap*. Vol. 57. Chapman and Hall, 436 pp.
- Gilleland, E., and R. W. Katz, 2016: extRemes 2.0: An extreme value analysis package in R. *J. Stat. Software*, **72** (8), <https://doi.org/10.18637/jss.v072.i08>.
- Harrison, D. L., S. J. Driscoll, and M. Kitchen, 2000: Improving precipitation estimates from weather radar using quality control and correction techniques. *Meteor. Appl.*, **7**, 135–144, <https://doi.org/10.1017/S1350482700001468>.
- Hawkins, E., D. Frame, L. Harrington, M. Joshi, A. King, M. Rojas, and R. Sutton, 2020: Observed emergence of the climate change signal: From the familiar to the unknown. *Geophys. Res. Lett.*, **47**, e2019GL086259, <https://doi.org/10.1029/2019GL086259>.
- Historic Environment Scotland, 2019: A guide to climate change impacts. Historic Environment Scotland Rep., 54 pp., www.historicenvironment.scot/archives-and-research/publications/publication/?publicationId=843d0c97-d3f4-4510-acd3-aadf0118bf82.
- Historic Environment Scotland, 2020: Edinburgh Castle. Historic Environment Scotland, <https://portal.historicenvironment.scot/designation/sm90130>.
- IPCC, 2021: Technical summary. *Climate Change 2021: The Physical Science Basis*, V. Masson-Delmotte et al., Eds., Cambridge University Press, 33–144.
- Karoly, D. J., and P. A. Stott, 2006: Anthropogenic warming of central England temperature. *Atmos. Sci. Lett.*, **7**, 81–85, <https://doi.org/10.1002/asl.136>.
- Kendon, M., M. McCarthy, S. Jevrejeva, A. Matthews, T. Sparks, J. Garforth, and J. Kennedy, 2022: State of the UK Climate 2021. *Int. J. Climatol.*, **42** (S1), 1–80, <https://doi.org/10.1002/joc.7787>.
- Met Office, 2003: Met Office rain radar data from the NIMROD system. NCAS British Atmospheric Data Centre, accessed 24 October 2023, <https://catalogue.ceda.ac.uk/uuid/82adec1f896af6169112d09cc1174499>.
- Met Office Hadley Centre, 2019: UKCP18 convection-permitting model projections for the UK at 2.2km resolution. NERC EDS Centre for Environmental Data Analysis, accessed 24 October 2023, <https://catalogue.ceda.ac.uk/uuid/ad2ac0ddd3f34210b0d6e19bfc335539>.
- Morice, C. P., and Coauthors, 2021: An updated assessment of near-surface temperature change from 1850: The HadCRUT5 data set. *J. Geophys. Res. Atmos.*, **126**, e2019JD032361, <https://doi.org/10.1029/2019JD032361>.
- National Academies of Sciences, Engineering, and Medicine, 2016: *Attribution of Extreme Weather Events in the Context of Climate Change*. National Academies Press, 186 pp.
- Parker, D. E., and E. B. Horton, 2005: Uncertainties in central England temperature 1878–2003 and some improvements to the maximum and minimum series. *Int. J. Climatol.*, **25**, 1173–1188, <https://doi.org/10.1002/joc.1190>.
- Phillips, H., 2014: Adaptation to climate change at UK World Heritage Sites: Progress and challenges. *Hist. Environ.*, **5**, 288–299, <https://doi.org/10.1179/1756750514Z.00000000062>.
- Pichelli, E., and Coauthors, 2021: The first multi-model ensemble of regional climate simulations at kilometer-scale resolution Part 2: Historical and future simulations of precipitation. *Climate Dyn.*, **56**, 3581–3602, <https://doi.org/10.1007/s00382-021-05657-4>.
- Reed, K., M. F. Wehner, A. M. Stansfield, and C. M. Zarzycki, 2021: Anthropogenic influence on Hurricane Dorian’s extreme rainfall. *Bull. Amer. Meteor. Soc.*, **102** (1), S9–S15, <https://doi.org/10.1175/BAMS-D-20-0160.1>.
- Reed, K., M. F. Wehner, and C. M. Zarzycki, 2022: Attribution of 2020 hurricane season extreme rainfall to human-induced climate change. *Nat. Commun.*, **13**, 1905, <https://doi.org/10.1038/s41467-022-29379-1>.
- Royal Meteorological Society, 2021: July 2021: Dry, sunny and warm in most of north and west. Often dull and wet much of central and eastern England; some notable thunderstorm deluges. *Weather*, **76**, i–iv, <https://doi.org/10.1002/wea.4068>.
- Saltikoff, E., and Coauthors, 2019: An overview of using weather radar for climatological studies: Successes, challenges, and potential. *Bull. Amer. Meteor. Soc.*, **100**, 1739–1752, <https://doi.org/10.1175/BAMS-D-18-0166.1>.
- Scottish Environment Protection Agency, 2020: The flash floods of 11 and 12 August 2020 in central and eastern Scotland. Scottish Environment Protection Agency Rep., 22 pp., www.sepa.org.uk/media/536333/the-flash-floods-of-11-and-12-august-2020.pdf.
- Tokarska, K. B., M. B. Stolpe, S. Sippel, E. M. Fischer, C. J. Smith, F. Lehner, and R. Knutti, 2020: Past warming trend constrains future warming in CMIP6 models. *Sci. Adv.*, **6**, eaaz9549, <https://doi.org/10.1126/sciadv.aaz9549>.
- Yamazaki, K., D. M. H. Sexton, J. W. Rostron, C. F. McSweeney, J. M. Murphy, and G. R. Harris, 2021: A perturbed parameter ensemble of HadGEM3-GC3.05 coupled model projections: Part 2: Global performance and future changes. *Climate Dyn.*, **56**, 3437–3471, <https://doi.org/10.1007/s00382-020-05608-5>.
- Yu, J., X.-F. Li, E. Lewis, S. Blenkinsop, and H. J. Fowler, 2020: UKGrSHP: A UK high-resolution gauge–radar–satellite merged hourly precipitation analysis dataset. *Climate Dyn.*, **54**, 2919–2940, <https://doi.org/10.1007/s00382-020-05144-2>.